

See discussions, stats, and author profiles for this publication at: <https://www.researchgate.net/publication/243374618>

# Nanostructures and Molecular Assembly of $\beta$ -Blocked Long Oligothiophenes up to the 96-Mer on Au (111) as Probed by in Situ Electrochemical Scanning Tunneling ...

ARTICLE in THE JOURNAL OF PHYSICAL CHEMISTRY C · AUGUST 2009

Impact Factor: 4.77 · DOI: 10.1021/jp9033276

---

CITATIONS

13

---

READS

32

## 5 AUTHORS, INCLUDING:



**Bernard John Vallejos Tongol**

University of Santo Tomas

11 PUBLICATIONS 71 CITATIONS

SEE PROFILE



**Li Wang**

Jiangxi Normal University

86 PUBLICATIONS 1,262 CITATIONS

SEE PROFILE



**Shuehlin Yau**

National Central University

93 PUBLICATIONS 1,881 CITATIONS

SEE PROFILE



**Kingo Itaya**

Tohoku University

246 PUBLICATIONS 8,355 CITATIONS

SEE PROFILE

# Nanostructures and Molecular Assembly of $\beta$ -Blocked Long Oligothiophenes up to the 96-Mer on Au(111) as Probed by in Situ Electrochemical Scanning Tunneling Microscopy

Bernard John V. Tongol,<sup>\*,†,‡,||</sup> Li Wang,<sup>†,#</sup> Shueh-Lin Yau,<sup>\*,‡,⊥</sup> Tetsuo Otsubo,<sup>§</sup> and Kingo Itaya<sup>\*,†,‡,||</sup>

Department of Applied Chemistry, Graduate School of Engineering, Tohoku University, Aoba-yama 04, Sendai 980-8579, Japan, Core Research Evolutional Science and Technology Organized by the Japan Science and Technology Agency (CREST-JST), Kawaguchi Center Building, 4-1-8 Honcho, Kawaguchi, Saitama 332-0012, Japan, and Department of Applied Chemistry, Graduate School of Engineering, Hiroshima University, Higashi-Hiroshima 739-8527, Japan

Received: April 10, 2009

The electrochemistry and adsorption of a series of  $\beta$ -blocked long oligothiophenes up to the 96-mer (96T) on Au(111) electrode were examined by using cyclic voltammetry (CV) and in situ electrochemical scanning tunneling microscopy (EC-STM), respectively, in 0.10 M HClO<sub>4</sub>. CV characterization presents the electrochemical behavior and stability of the oligothiophene-modified Au(111) in aqueous perchloric acid solution. EC-STM characterization revealed lamella-type molecular arrangement with the molecular axis aligned along the main crystallographic axis of the Au(111) substrate. High-quality STM molecular resolution imaging was obtained to reveal details of conformation, dimension, and packing habit of the oligothiophene nanostructures.

## Introduction

The superior electronic and transport properties of conjugated polymers and oligomers have rendered their applications to fabricate organic electronic devices, such as light-emitting diodes (LEDs), field-effect transistors (FETs), photovoltaic cells, etc.<sup>1,2</sup> The structure of the molecular assembly at solid surfaces can be critical to the performance of these molecular devices.<sup>3,4</sup> To understand how the structure of oligo- and polythiophene molecules affect their conductivity, researchers have designed and synthesized many thiophene derivatives and characterized their arrangements on the basal plane of HOPG or MoS<sub>2</sub> by using scanning tunneling microscopy (STM).<sup>5,6</sup> Highly ordered molecular adlayers have been frequently observed, which are presumed as physisorbed systems. The molecule–substrate interaction is believed to be so weak that it barely affects how thiophene molecules interact with one another. In other words, STM can be a simple and straightforward tool to probe the packing of oligothiophene molecules in the form of bulk crystals.<sup>5b</sup> STM was also used to examine poly(3-alkylthiophenes) adsorbed on Au(111) surface, revealing a largely disordered structure.<sup>7a</sup> Substituent effect of short oligothiophenes on Au(111) was investigated using in situ STM<sup>7b</sup> while direct

conformational analysis of 10 nm oligothiophene nanowire was studied using UHV-STM on Au(111).<sup>7c</sup>

Extended  $\alpha$ -conjugated oligothiophenes have been studied for a decade to shed an insight into the extent of conjugation in polymeric materials. With the  $\beta$ -positions of thiophene unit blocked by a fused cyclopentane ring, thiophene molecules undergo oxidative coupling to produce chemically pure thiophene up to the 96-mer (96T).<sup>8</sup> The chemical structure of 96T molecule is shown in Figure 1. It has been shown that 96T affords the longest  $\pi$ -conjugation, which exceeds the value extrapolated from results obtained for 20-mer. The adsorption and crystallization of 96T on solid support, which can be important to inform molecular arrangement in bulk crystals and to apply this molecule in molecular electronics, have not been examined thus far. This article is devoted to the electrochemistry and STM studies of a series of long, well-defined oligothiophenes, namely, 24-mer (24T), 48-mer (48T), and 96-mer (96T) on Au(111) electrode in 0.10 M HClO<sub>4</sub>.

We are able to acquire high-quality STM molecular resolution imaging to address the conformation and packing habit of 24T, 48T, and 96T nanostructures on Au(111) surface.

## Experimental Section

The undoped 24T, 48T, and 96T samples, previously synthesized, purified, and characterized by physical methods,<sup>8</sup> were obtained from Prof. Otsubo's laboratory and were used as received. Au(111) single-crystal electrodes were prepared by the Clavilier method<sup>9</sup> and were finally annealed in a hydrogen flame and quenched into ultrapure water (Milli-Q SP-TOC;  $\geq 18.2$  M $\Omega$  cm) saturated with hydrogen to obtain Au(111)-( $\sqrt{3} \times 22$ ).<sup>10</sup> The oligothiophene adlayer was formed by immersing the clean Au(111) electrode into a  $\sim 10$   $\mu$ M benzene solution of the oligothiophene sample (e.g., 96T) for 30 s, unless otherwise stated. The obtained 96T-modified Au(111) electrode was air-dried under N<sub>2</sub> and transferred immediately into an electrochemical cell containing 0.10 M HClO<sub>4</sub> solution for CV

\* Corresponding authors and current affiliations. E-mail: bvtongol@mml.ust.edu.ph. Tel/Fax: (63-2) 7314031; E-mail: yau6017@ncu.edu.tw. Tel: 886-3-4279573. Fax: 886-3-4227664. E-mail: itaya@atom.che.tohoku.ac.jp.

<sup>†</sup> Tohoku University.

<sup>‡</sup> CREST-JST.

<sup>⊥</sup> Hiroshima University.

<sup>||</sup> Current address: Department of Chemistry, College of Science and Research Center for the Natural Sciences, University of Santo Tomas, Espana, 1015 Manila Philippines.

<sup>#</sup> Present address: Department of Chemistry, National Central University, 300 Jongda Road, Zhongli, Taoyuan, Taiwan 320 ROC.

<sup>§</sup> Current address: College of Chemistry and Chemical Engineering, Jiangxi Normal University, Nanchang 330022, China

<sup>||</sup> Current address: WPI Advanced Institute for Materials Research, Tohoku University.

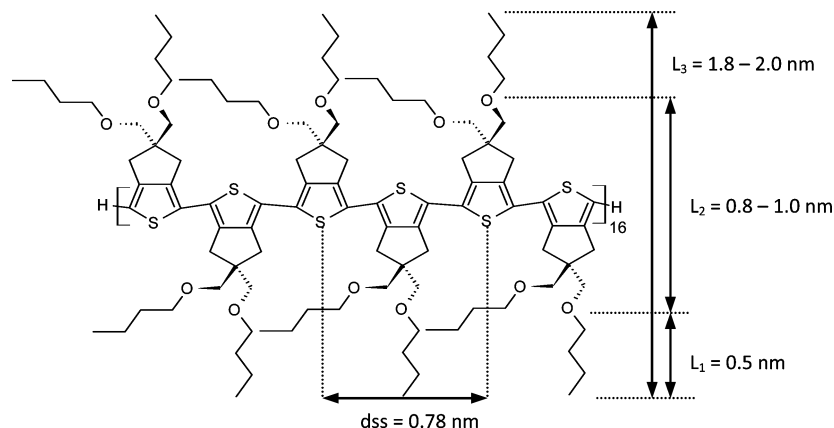


**Figure 1.** Chemical structure of an idealized chain fragment of 96T. The related respective intrachain distances ( $L_1$ ,  $L_2$ ,  $L_3$ , and  $D_{ss}$ ) are estimated from calculations using the Chemschetch (version 5.06) and 3D (version 5.07) software packages (Advanced Chemistry Development Inc., Toronto, Ontario M5H 3 V9, Canada).

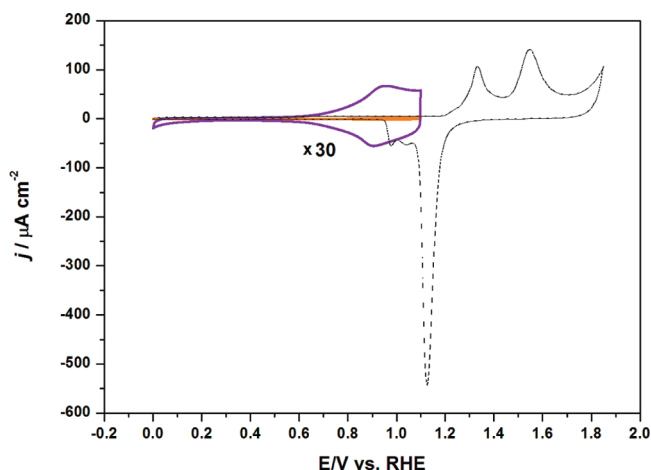


**Figure 2.** (a) Typical cyclic voltammograms of bare (dotted line) and 96T-modified (solid line) Au(111) electrodes in 0.10 M  $\text{HClO}_4$ . The scan rate was  $50 \text{ mV} \cdot \text{s}^{-1}$ . The purple line shows the expanded (30 times) CV of 96T adlayer.

and EC-STM measurements. The in situ EC-STM was performed with a Nanoscope E (Digital Instruments, Santa Barbara, CA) operated in a constant current mode. The tungsten tip used was electrochemically etched in 1 M KOH and painted with nail polish to minimize the residual faradic current. Cyclic voltammetry was performed with Au(111) electrode positioned in the hanging meniscus configuration in a three-compartment cell. All potentials were referred to the reversible hydrogen electrode (RHE) in 0.10 M  $\text{HClO}_4$ .

## Results and Discussion

**Electrochemistry of a Series of  $\beta$ -Blocked Oligothiophenes up to 96-Mer (96T) on Au(111).** Figure 2 shows typical cyclic voltammograms (CVs) recorded at  $50 \text{ mV} \cdot \text{s}^{-1}$  scan rate for well-ordered Au(111) electrodes with (solid trace) and without (dotted trace) a 96T adlayer in 0.10 M  $\text{HClO}_4$ . The characteristics of the dotted trace are identical to that reported for an electrochemically clean Au(111) electrode.<sup>10</sup> The 96T-modified Au(111) electrode produces a featureless  $i$ - $V$  profile between 0 and 0.50 V, and an oxidation peak at 0.95 V in the positive scan to 1.1 V. The latter feature is ascribed to the doping process. On the reverse sweep from 1.1 to 0 V, one peak emerged at 0.91 V, which could be associated with the undoping process of the oligomer, accordingly. These thoughts are based on conclusions of previous studies on oligothiophene.<sup>11</sup> During doping at 0.95

V, the  $\text{ClO}_4^-$  inserts into the polymer backbone balancing the charges in the system. The  $\text{ClO}_4^-$  exits the polymer backbone during undoping at 0.91 V (Figure 3). The doping and undoping process is also attributable to the formation of different charge carriers in the two doping states, positive polarons, bipolarons and free carriers in p-doping and only negative polarons in n-doping.<sup>11d</sup>

Extensive CV studies demonstrate that the 96T-modified Au(111) electrode can be repeatedly cycled between 0.0 and 1.10 V (vs RHE) (Figure 3c, curve 1 with the heaviest or darkest curve trace) without any apparent loss of electroactivity even after more than five scan cycles. Increasing the upper positive potential limit (Figure 3c, curves 2–4, with decreasing weight or intensity of the curve trace) leads to higher redox charges,  $Q$ , with relatively stable voltammograms for five cycles or even more in each of the curve trace. The  $Q$  value includes both faradaic and capacitive contributions. It is interesting to note that the reverse sweep from 1.1 to 0 V produced a two-component cathodic peak. To understand the nature of the cathodic peak, we performed CV characterization of 24T and 48T, shorter oligomer fragments of 96T, which were also chemically synthesized by Otsubo's group<sup>8</sup> (Figure 3, panels a and b). Apparently, the reductive process (i.e., undoping or discharging) in the oligomer can be one-component or two-component depending on the experimental parameters or conditions (e.g., concentration of the oligomer, deposition time, and potential cycling). The asymmetry between the doping and the undoping process in the CVs of Figure 3, panels a and c, could be attributed to structural relaxation and conformational changes,<sup>11b,12a</sup> distinct oxidation stages with modification in the interaction among charged sites,<sup>12b,c</sup> and differences in the properties of the oxidized and neutral oligomer.<sup>12d</sup>

The occurrence of a two-component cathodic process is characterized by a main wave with a narrower to sharper reductive peak followed by a small peak or a shoulder at a potential 15–20 mV less positive than the main reductive peak. This small peak could be the result of hysteresis in the reduction of charged species deposited on the electrode in the anodic scan.<sup>12e</sup> A strong potential hysteresis is a common feature of solid-state voltammograms of many conjugated systems. In agreement with the present study, hysteresis effects in oligothiophenes are not observed until a certain potential or charging level is exceeded.<sup>12e</sup>

**Molecular Assembly of Long Oligothiophenes on Au(111) Substrate.** Typical large scale STM images are revealed for 24T- (Figure 4a), 48T- (Figure 4b), and 96T-modified (Figure

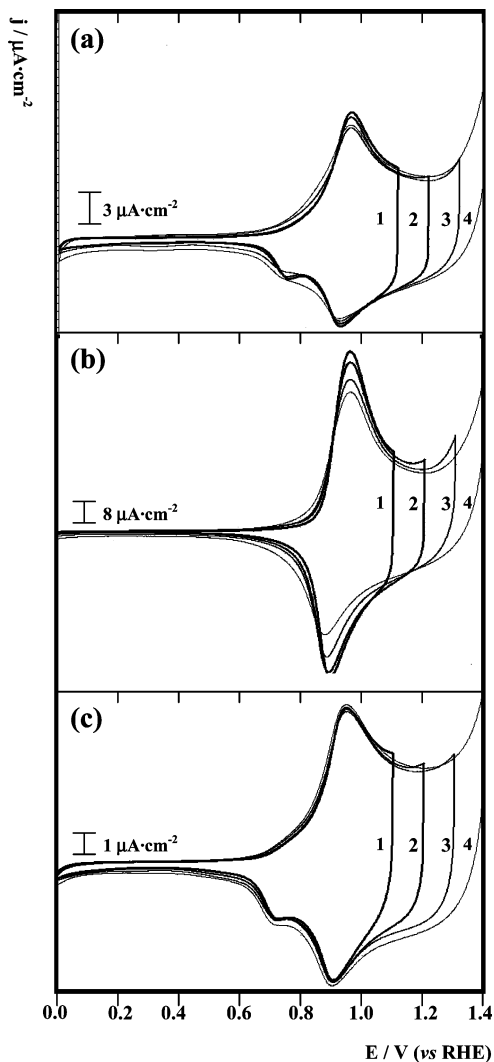


**Figure 3.** Electrochemical behavior of a series of novel, undoped oligothiophenes: (a) 24T, (b) 48T, and (c) 96T coated on Au(111) electrode in 0.10 M HClO<sub>4</sub> at a scan rate,  $\nu = 50 \text{ mV} \cdot \text{s}^{-1}$ . Immersion or deposition time in  $10^{-4}$  M oligomer solution was 5 min in all cases. Increase in potential cycling is indicated by the numbered curves 1–4 and by decreasing intensity or weight in the curve trace.

4c) Au(111) electrodes at 0.25 V (vs RHE) in 0.10 M HClO<sub>4</sub>. The novel oligothiophene adlayers were imaged as extended bright fine lines<sup>13</sup> with their conjugated backbones aligned parallel to the close-packed atomic directions of the Au(111) substrate. Indeed, STM spotted three differently aligned ad-molecules, as expected for the 3-fold symmetry of Au(111) substrate.

Extensive STM imaging effort reveals that the backbone chains of these oligothiophene adlayers were mostly linear with minor deformations of bending and folding. Within molecular aggregates, the conjugated skeletons of these oligomers are stacked in lamellar patterns, which afforded close packing and possibly efficient electronic coupling.<sup>5c,d</sup> Likewise, these adlayers were potential dependent. The molecular arrangements seen in Figure 4a–c were stable between 0.05 to 0.50 V, but switching the potential beyond this range caused drastic restructuring of the adlayer. More specifically, possible desorption and oxidation of the ad molecules commenced at potentials negative of 0.05 V and positive of 0.50 V, respectively. Beyond this potential range, the adsorbed oligothiophenes are mobile and hence cannot be imaged by STM. Switching back to the double-layer potential of 0.25 V, the adlayer structures reappeared after several

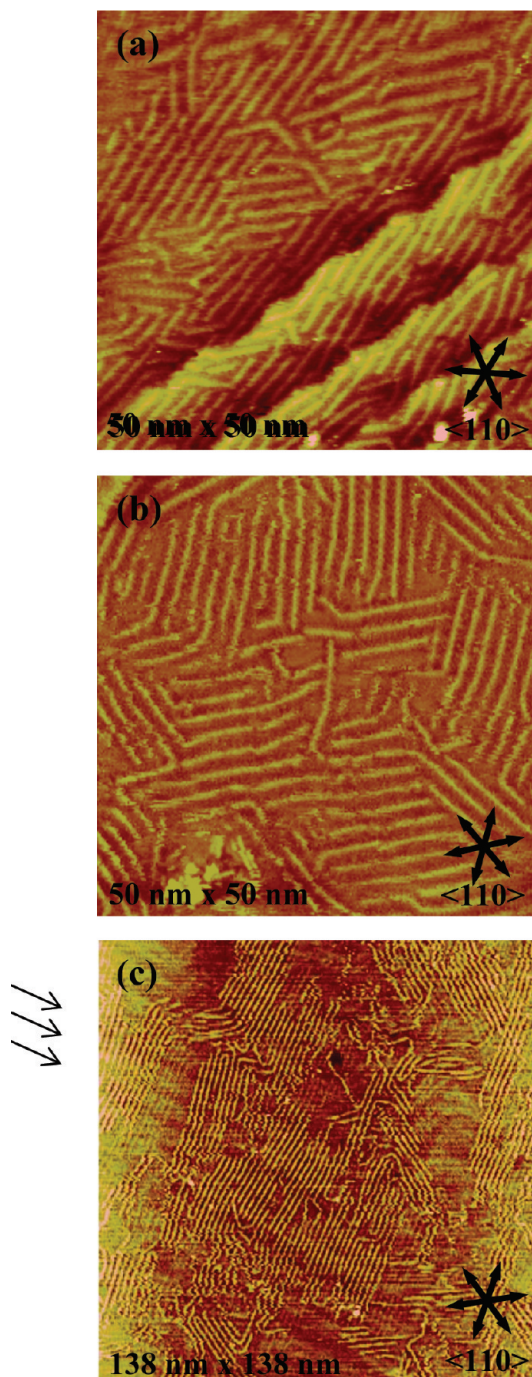


**Figure 4.** STM images of (a) 24T-, (b) 48T-, and (c) 96T-modified Au(111) electrodes at  $E = 0.25 \text{ V}$  (vs RHE) in 0.10 M HClO<sub>4</sub>. Tunneling parameters are  $V_B = -107 \text{ mV}$  and  $I_T = 300 \text{ pA}$  for (a),  $V_B = 165 \text{ mV}$  and  $I_T = 200 \text{ pA}$  for (b), and  $V_B = -150 \text{ mV}$  and  $I_T = 2 \text{ nA}$  for (c). The set of three arrows at the bottom right indicates the close-packed directions of the Au(111) substrate. The black arrows at the left of (c) indicate the reconstruction lines of Au(111).

minutes, but in smaller domains and less perfectly ordered. At this point, we did not attempt to image beyond this potential since we could not obtain reproducible STM images. From Figure 2, oxidation of the oligomers begins at around 0.7 V until it is fully oxidized at around 0.95 V, creating positive charges (radical cation, dication, etc.) with increasing electrode potential.<sup>11</sup> Oxidative desorption of oligothiophenes on Au(111) could possibly take place, but a detailed mechanistic study of the dynamics of adsorption–desorption are difficult to follow with the time scale of our STM analysis. Thus, the electrode



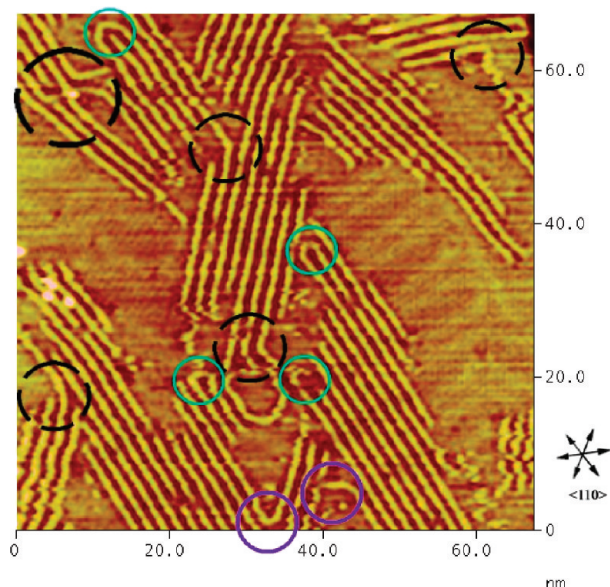


**Figure 5.** Submolecular resolution STM image of a 96T adlayer formed on Au(111) acquired at 0.25 V in 0.10 M HClO<sub>4</sub>. Single oligothiophene chain can be discerned in this STM image. Some typical chain folding and bent conformations are indicated by colored circle (hairpin folding by green circle, 120° bending by black circle and 60° bending by purple circle).

potential was positioned within the double layer potential region to obtain ordered oligothiophene adlayers.

The chain lengths of the oligomers were statistically measured from the STM images and evaluated to be  $10.60 \pm 2.07$ ,  $16.11 \pm 1.68$ , and  $36.00 \pm 1.83$  nm for 24T, 48T, and 96T, respectively. Assuming that it adopts an energetically favorable all-trans conformation with regards to the thiophene-ring linkage, 96T is estimated to have a chain length of 37.2 nm.<sup>8</sup> It follows that 24T and 48T would have chain lengths of 9.3 and 18.6 nm, respectively. These computed chain lengths are based on theoretical calculations<sup>14</sup> and are in close agreement with the chain lengths derived and measured from the STM images (Figure 4a–c).

On the other hand, close inspection of Figure 4c shows that the adsorption of 96T apparently did not lift the reconstructed Au(111) surface, as the herringbone characteristics were clearly discerned as stripes running from the upper left to the lower right of the STM image. Moreover, the 96T ad molecules frequently crisscrossed the herringbone structure perpendicularly or were aligned perpendicular to the  $\langle 112 \rangle$  direction of Au(111) surface.

It is interesting to note that in the early stage of adsorption process, the adsorption of individual chains and smaller aggregates onto the Au(111) surface may result in predominantly parallel lamellae. Because of the bulky and long side-chains, this series of  $\beta$ -blocked oligothiophenes has a greater tendency to form aggregates<sup>5c</sup> (most likely evident in the lower left image of Figure 4b). In this regard, they were used in lower concentration (i.e.,  $\sim 10 \mu\text{M}$ ) and at shorter immersion time (i.e.,  $\sim 30$  s). However, individual chains also seem to fold back quite regularly and bend at certain angles without loss of interaction energy. After most parts of the surface are covered, macromolecules from the solution can only adsorb onto open areas and in the remaining gaps by regular folding of 180° (most specifically evident in Figure 4c) and random bending at angles of 60° or 120° (Figure 4a–c).

Figure 5 reveals a higher resolution STM scan, which highlights the bending and folding deformations of 96T. A few

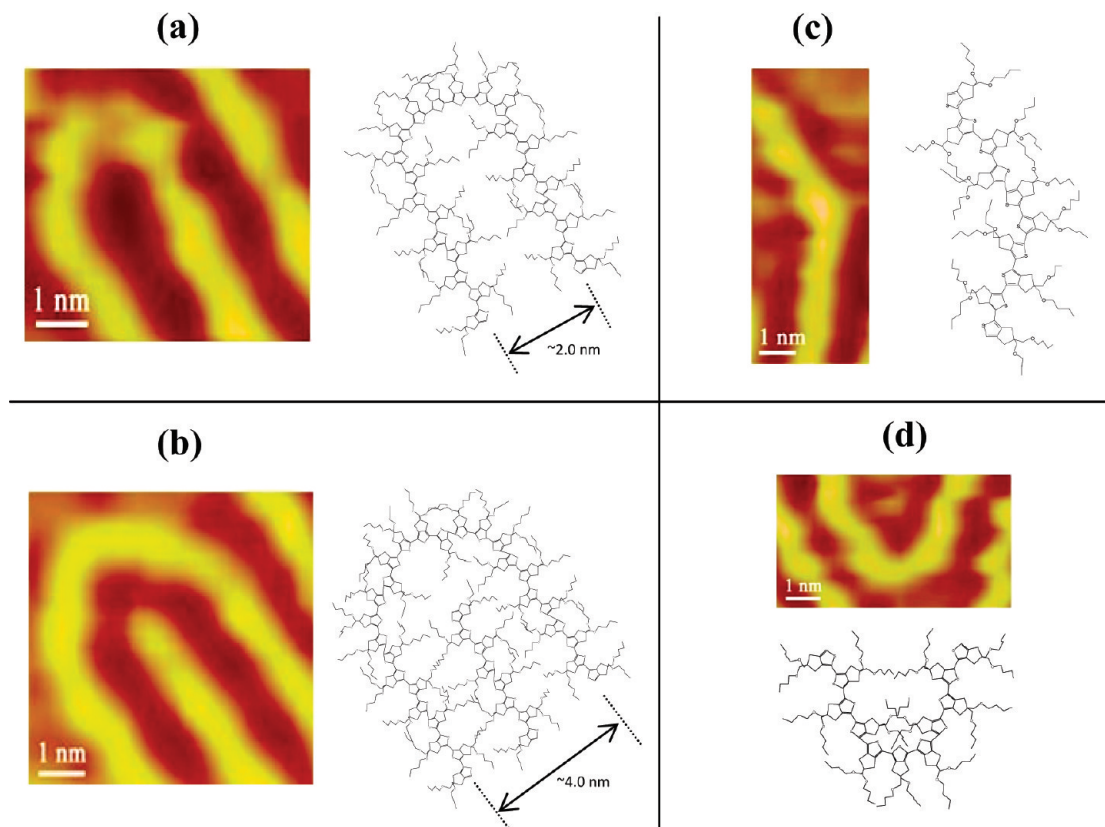
shorter fragments were also spotted, and are attributed to some shorter oligothiophene contained in the sample of 96T.<sup>8</sup> The linear conformation of 96T implied an all-trans conformation, the most favorable structure of polythiophene molecules.<sup>8</sup> Meanwhile, this image reveals some folded (encircled in green) and bent (encircled in black and purple) polymeric chains as indicated in Figure 5. Regular hairpin type of folding usually appeared within a lamella, while bent conformations, either at 120° or 60°, mostly emerged at boundaries between lamella. Similar long chain folding was reported by others.<sup>5c–e</sup>

To simulate the STM images, the structures of 96T fragments depicting the molecular folds and bends are proposed using molecular modeling. A 3-D optimization of the molecular structures was employed based on modified molecular mechanics.<sup>14</sup> The calculations were performed such that the first chain fragments of at least four thiophene units have been optimized in an all-trans or an all-cis conformation, the interaction of two strands was calculated subsequently, and finally the fragments were assembled in order to construct the oligomer chains and to simulate the STM images in Figure 5. (Molecular mechanics calculations are somewhat similar to Figure 2, ref 15)

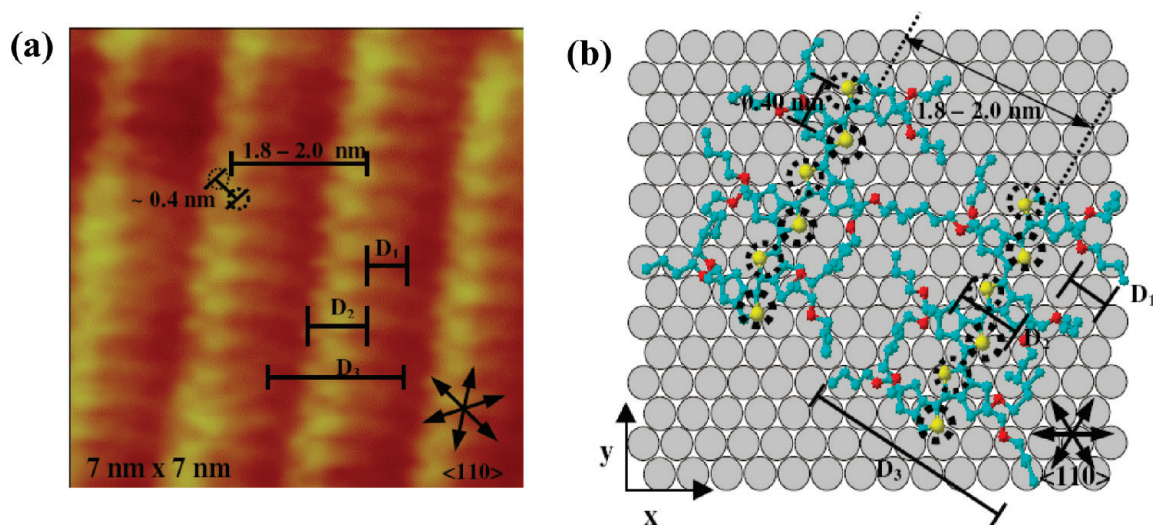
Statistically, bending at 120°, 60°, and irregular angles accounts for 65, 10, and 5% of the nonlinear molecular conformations, respectively, while hairpin type folding makes up the remaining 20%. Figure 6 presents models to explain these deformations of 96T.<sup>14</sup> Normally, 96T is expected to adopt an all-trans configuration, but it is necessary to switch to cis conformations at the elbows of bending or folding, as this would reduce steric hindrance between neighboring thiophene units.<sup>5c</sup> The hairpin type folding could be best explained by including seven consecutive thiophene units arranged in an all-cis conformation (Figure 6a), whereas folding in larger curvatures in a form of paperclip could involve multiple cis–trans conformations (Figure 6b). We propose that the 120° and 60° bending involved two and three consecutive cis-conformation of the thiophene units (Figure 6, panels c and d), respectively.<sup>14</sup>

Figure 7a presents a close-up view ( $7 \times 7 \text{ nm}^2$ ) of the 96T monolayer on Au(111), which reveals alternating bright and dark stripes running along the  $\langle 110 \rangle$  direction of the Au(111) surface and the proposed molecular model (Figure 7b). The bright stripes are readily associated with the backbones of 96T. Close scrutiny of the bright stripes discloses “sawtoothed” edge structures as represented by dashed circles in the STM image. The brighter spots (dashed circles with darker trace), with characteristic tailing, are more elevated than those of the lighter spots (dashed circles with lighter trace). Although noise in the imaging obfuscated these features, the two neighboring spots (i.e., light and bright spots) gave a distance of ca. 0.40 nm. This value ( $\sim 0.40$  nm) agrees with the sulfur–sulfur distance of two neighboring thiophene rings and also with the sulfur–sulfur distance  $d_{ss}$  in a triad (0.78 nm; Figure 1) as supported by theoretical calculation<sup>14</sup> and as reported previously for PHT films.<sup>5d</sup> Thus, these ragged features can be ascribed to thiophene rings or thiophene monomer units arranged in all-trans configuration. Though it is tempting to associate the tailing in the brighter spots with the side-chains, they are not imaged clearly with STM. They are most likely located within the trenches.

It is emphasized that this molecular resolution image provides some important measurements of 96T molecules, as these results are used to infer how 96T were stacked on the Au(111) substrate. The values of  $D_1$ ,  $D_2$ , and  $D_3$  marked in Figure 7 are 0.5, 0.8, and 1.8 nm, respectively, which correspond to the half-width of dark stripe, the width of bright stripe, and the spacing between two nearest neighbors of 96T, respectively. They are



**Figure 6.** STM images depicting the (a) hairpin and (b) paperclip folding and (c) 120° and (d) 60° bending in 96T with their corresponding proposed molecular models.



**Figure 7.** (a) High-resolution STM image ( $7 \times 7 \text{ nm}^2$ ) of 96T adlayer on Au(111) substrate at 0.25 V in 0.10 M  $\text{HClO}_4$  and (b) corresponding molecular model of two parallel linear strands of 96T adlayer on Au(111) surface (colored gray for better contrast). Tunneling parameters:  $V_B = -320 \text{ mV}$ ;  $I_T = 400 \text{ pA}$ .

well consistent with the length of the butoxy side chain ( $L_1$ ), the width of 96T conjugated backbone ( $L_2$ ), and the dimension of 96T molecule ( $L_3$ ; Figure 1).<sup>14</sup> These results strongly suggest that the alkyl side chains of 96T molecules were fully extended on the substrate, and they did not interdigitate (Figure 7b). Moreover, the 96T molecules arrange themselves close-packed with the neighboring molecules. The structural parameters of 96T are also true for 24T and 48T with their surface coverage almost similar, indicating that the adlayers of these oligothiophenes are close-packed on the Au(111) surface.

Several STM studies<sup>7</sup> have shown that the sulfur atoms in the thiophene units and thiophene backbone have strong

interaction with the Au(111) substrate. Noh and co-workers<sup>7d</sup> have observed that in the case of thiophene self-assembled monolayers (SAMs), the sulfur head-groups in thiophene are adsorbed at various adsorption sites of the Au(111) lattice. Moreover, a cofacial interaction between thiophene molecules plays an important role in the self-assembly process on Au(111). In addition, it is considered that thiophene molecules at saturation coverage are arranged with an upright configuration with the tilt angle of approximately  $18^\circ$  from the surface normal.<sup>7d</sup> Meanwhile, the effects of chain length and substituents on the oligothiophene adlayer structures were also seen from the STM images.<sup>7b,c</sup> Wan's group<sup>7b</sup> reported the adlayer



structures of short oligothiophenes with alkyl substituents and carboxyl groups at terminal thiophene units. Highly ordered long-range adlayer structures were seen on Au(111) for bithiophene and terthiophene, indicating strong molecule–molecule interaction via hydrogen bonding. Moreover, the oligothiophene adlayers were aligned parallel on the main crystallographic axes of Au(111). Quaterthiophene form short-range ordered structure with hexagonal symmetry while disordered pattern is observed on pentathiophene adlayer due to its strong substrate-molecule interaction.<sup>7b</sup> Meanwhile, long oligothiophene 24-mer, substituted with N-silyl groups and dodecyl side-chains, was investigated by Yokoyama's group<sup>7c</sup> using UHV-STM. The adlayer structure revealed conformational variations of straight and bent chains in the 10 nm oligothiophene nanowire. The conformational variations are influenced by solvent and substituents. These STM studies of thiophene and thiophene derivatives on Au(111) substrate could explain the surface interaction between Au(111) substrate and sulfur atoms of the oligothiophenes. Apparently, 24T, 48T, and 96T admolecules were aligned along the main axis of Au(111) with no side-chain interdigitation, indicating predominance of substrate-molecule interaction.

## Conclusions

The electrochemistry of the newly synthesized  $\beta$ -blocked long oligothiophenes has been studied using cyclic voltammetry on Au(111) electrode in 0.10 M HClO<sub>4</sub> electrolyte solution. The oligothiophene-modified Au(111) electrodes have oxidation potential of  $E = 0.95$  V (vs RHE) with observed stability to potential cycling in aqueous perchloric acid electrolyte solution. With regards to structural elucidation, the adsorption of 24T, 48T, and 96T on Au(111) electrode has been probed by using in situ EC-STM revealing a lamella-type arrangement with no side-chain interdigitation. The backbones of these novel oligothiophenes are preferentially aligned along the main axis of the Au(111) surface. High-resolution STM imaging reveals the internal molecular structures of 96T, which are mostly linear with thiophene units arranged in an all-trans configuration. Bending and folding conformations were also observed, which involve cis-configuration at curved regions. The structural parameters of 96T are also true for 24T and 48T with their surface coverage almost similar, indicating that the adlayers of these oligothiophenes are close-packed on the Au(111) surface. This information is useful to understand how oligothiophene with long backbone like 96T would arrange on solid support, a critical step toward the utility of conducting polymers in plastic and molecular electronic devices with enhanced performance.

**Acknowledgment.** This work was supported partly by the Core Research for Evolutional Science and Technology (CREST)

organized by Japan Science and Technology Agency (JST) during the period of 2002–2008, and partly by the New Energy and Industrial Technology Development Organization (NEDO). The Ministry of Education, Culture, Sports, Science and Technology, Japan and the Center of Excellence (COE) Project on Giant Molecules and Complex Systems are also gratefully acknowledged.

## References and Notes

- (1) Handbook of Oligo- and Polythiophenes. Fichou, D., Ed.; Wiley-VCH: Weinheim, 1998.
- (2) Electronic Materials: The Oligomer Approach. Mullen, K.; Wegner, G., Eds.; Wiley-VCH: Weinheim, 1998.
- (3) Sirringhaus, H.; Brown, J. P.; Friend, R. H.; Nielsen, M. M.; Bechgaard, K.; Langeveld-Voss, B. M. W.; Spiering, A. J. H.; Janssen, R. A. J.; Meijer, E. W.; Herwig, P.; de Leeuw, D. M. *Nature* **1999**, *401*, 685.
- (4) Hoofman, R. J. O. M.; de Haas, M. P.; Siebbeles, L. D. A.; Warman, J. M. *Nature* **1998**, *392*, 54.
- (5) (a) Bauerle, P.; Fischer, T.; Bidlingmeier, B.; Stabel, A.; Rabe, J. P. *Angew. Chem., Int. Ed. Engl.* **1995**, *34*, 303. (b) Azumi, R.; Gotz, G.; Debaerdemaeker, T.; Bauerle, P. *Chem.—Eur. J.* **2000**, *6*, 735. (c) Mena-Osteritz, E.; Meyer, A.; Langeveld-Voss, B. M. W.; Janssen, R. A. J.; Meijer, E. W.; Bauerle, P. *Angew. Chem., Int. Ed. Engl.* **2000**, *39*, 2679. (d) Grevin, B.; Rannou, P.; Payerne, R.; Pron, A.; Travers, J. P. *J. Chem. Phys.* **2003**, *118*, 7097. (e) Brun, M.; Demadrille, R.; Rannou, P.; Pron, A.; Travers, J. P.; Grevin, B. *Adv. Mater.* **2004**, *16*, 2087. (f) Mena-Osteritz, E. *Adv. Mater.* **2002**, *14*, 609, and references therein.
- (6) Azumi, R.; Gotz, G.; Bauerle, P. *Synth. Met.* **1999**, *101*, 569.
- (7) (a) Kaneto, K.; Harada, K.; Takashima, W.; Endo, K.; Rikukawa, M. *Jpn. J. Appl. Phys.* **1999**, *38*, L1062. (b) Wang, L.; Yan, H.-J.; Wan, L.-J. *J. Nanosci. Nanotechnol.* **2007**, *7*, 3111. (c) Nishiyama, F.; Ogawa, K.; Tanaka, S.; Yokohama, T. *J. Phys. Chem. B* **2008**, *112*, 5272. (d) Noh, J.; Ito, E.; Nakajima, K.; Kim, J.; Lee, H.; Hara, M. *J. Phys. Chem. B* **2002**, *106*, 7139.
- (8) Izumi, T.; Kobashi, S.; Takimiya, K.; Aso, Y.; Otsubo, T. *J. Am. Chem. Soc.* **2003**, *125*, 5286.
- (9) Clavilier, J.; Faure, R.; Guinet, G.; Durand, R. *J. Electroanal. Chem.* **1980**, *107*, 205–209.
- (10) Honbo, H.; Sugawara, S.; Itaya, K. *Anal. Chem.* **1990**, *62*, 2424.
- (11) (a) Roncali, J.; Giffard, M.; Jubault, M.; Gorgues, A. *J. Electroanal. Chem.* **1993**, *361*, 185. (b) Tourillon, G.; Garnier, F. *J. Electroanal. Chem.* **1984**, *161*, 51. (c) Domagala, W.; Lapkowski, M.; Guillerez, S.; Bidan, G. *Electrochim. Acta* **2003**, *48*, 2379. (d) Skompska, M.; Mieczkoski, J.; Holze, R.; Heinze, J. *J. Electroanal. Chem.* **2004**, *577*, 9.
- (12) (a) Heinze, J.; Bilger, R.; Meerholz, K. *Ber. Bunsen-Ges. Phys. Chem.* **1988**, *92*, 1266. (b) Zotti, G.; Schiavon, G. *Synth. Met.* **1989**, *31*, 347. (c) Marque, P.; Roncali, J. *J. Phys. Chem.* **1990**, *94*, 8614. (d) Chao, F.; Costa, M. *Synth. Met.* **1990**, *39*, 97. (e) Meerholz, K.; Heinze, J. *Electrochim. Acta* **1996**, *41*, 1839.
- (13) Fisher, J.; Blochl, P. E. *Phys. Rev. Lett.* **1993**, *70*, 3263.
- (14) The related molecule parameters are estimated from calculations using the ChemsSketch (version 5.06) and 3D (version 5.07) software packages (Advanced Chemistry Development Inc., Toronto, Ontario M5H 3 V9, Canada).
- (15) Kasai, H.; Tanaka, K.; Okada, S.; Oikawa, H.; Kawai, T.; Nakanishi, H. *Chem. Lett.* **2002**, 696–697.

JP9033276